Multifunctional ultralight, recoverable, piezoresistive, and super thermal insulating SiC nanowire sponges

Yu Chen[1,2], Lei Han[2,3], Oluwafunmilola Ola[4], Guangsheng Liu[1], Nannan Wang[1,*], Zakaria Saadi[2], Ana I. S. Neves[2], Rana Sabouni Tabari[2], Kunyapat Thummavichai[2], Ahmed M. E. Khalil[2], Yongde Xia[2], Shibin Sun[5], Yanqiu Zhu[1,2,*]

[1]GIFT (Guangxi Institute for Fullerene Technology), School of Resources, Environment and Materials, Guangxi University, Guangxi 530004, China

[2]College of Engineering, Mathematics and Physical Sciences, University of Exeter, Exeter, EX4 4SB, UK

[3]The State Key Laboratory of Refractories and Metallurgy, Wuhan University of Science and Technology, Wuhan, 430081, China

[4]Advanced Materials Group, Faculty of Engineering, The University of Nottingham, Nottingham, NG7 2RD, United Kingdom

[5]College of Logistics Engineering, Shanghai Maritime University, Shanghai, 201306, China

*Corresponding author.

E-mail: Y.Zhu@exeter.ac.uk; wangnannan@gxu.edu.cn

Abstract

Ultralight three-dimensional (3D) architectured silicon carbide (SiC) nanowire sponges with integrated properties of recoverable compressibility, outstanding high-temperature thermal and chemical stability, and fire-retardance have been actively pursued in recent years.

This article has been accepted for publication and undergone full peer review but has not been through the copyediting, typesetting, pagination and proofreading process, which may lead to differences between this version and the Version of Record. Please cite this article as doi: 10.1111/jace.18823.

However, efficient construction of SiC nanowire sponges with well-controlled overall shapes and distribution of SiC nanowires remains challenging. Herein, by coupling the electrospinning technique and carbothermal reduction process, we have developed a new fabrication process for highly porous and free-standing 3D SiC nanowire (SiCNW) sponges with closely attached nanowires through thermal treatment of stacked electrospun PAN/SiO_2 nanofibre membranes. The resulting SiCNW sponges possess ultralow density (~29 mg cm^{-3}), excellent compressive recoverability from large compressive deformation (up to 40% strain), and fatigue resistance, which endow them with excellent piezoresistive sensing capability under a variety of complex conditions. Furthermore, the sponges display superb thermal insulation (thermal conductivity of 24 mW $m^{-1}K^{-1}$) and fire-retardance. We believe that the present process provides technical clues for the development of other multifunctional ceramic sponges, and that further development of these ultralight multifunctional ceramic sponges offers potential for the design of advanced components for application in harsh engineering environments.

Keywords

SiC nanowire sponge, electrospinning, carbothermal reduction, piezoresistive sensor, thermal insulation

1. Introduction

SiC sponges that consist of interconnected flexible SiCNWs could exhibit outstanding elasticity, excellent high-temperature chemical stability, superb thermal insulation behaviour

and fire retardance, making them promising for applications operating under extreme conditions.[1]

One of the most common approaches for the fabrication of SiCNWs is direct carbothermal reduction of SiO_2.[2] As the carbothermal reaction is a slow gaseous process, chemical vapor deposition (CVD) has therefore emerged as an attractive approach for the fabrication of 3D SiCNW networks. Su et al. prepared ultralight and recoverable SiCNW aerogel by a facile CVD method on a graphite substrate, and the paper-like SiCNW aerogel was then detached and stacked together layer by layer to form a free-standing 3D SiCNW aerogel.[3,4] To accelerate the fabrication process, Li et al. directly deposited SiCNWs on a 3D substrate.[5] However, in this approach, the SiCNWs were generated from the surface of the template, easily causing uncontrolled growth and inhomogeneous distribution of SiCNWs, leading to limited structural stability. Moreover, the template-based CVD method requires both template preparation and removal after the deposition process, which considerably reduces the production efficiency.

Spinning technique as a common method for the production of 1D nanowires is then considered as an alternative since the preparation of SiCNWs by thermal treatment of electrospun polycarbosilane,[6-8] or polymer-SiO_2 mixture nanofibers[9,10] has been well established. However, due to the limitation of the spinning technique, electrospun fibres are just loosely accumulated naturally on the collector as random or oriented nanofibers with poor interconnection, which are considered unsuitable for generating large-scale 3D networks with regular shapes.[11,12] Therefore, additional freeze-casting technique was commonly utilised to assemble the randomly piled SiCNWs into 3D networks.[13] Unfortunately, the

complex procedure, stringent requirement for equipment, large cryogenic energy consumption, and high cost have limited the practical use of freeze-casting.[14]

Herein, we have developed a cost-effective, rapid, and flexible manufacturing approach for the fabrication of ultralight 3D SiCNW sponges by one-step sintering of stacked and compacted electrospun PAN/SiO_2 nanofibre membranes. The SiCNWs generated by carbothermal reduction process will be bonded together closely with each layer in the 3D structures. We have investigated thoroughly the microstructural features, recoverable compressibility, and fatigue resistance of SiCNW sponges and demonstrated their multifunctionalities such as piezoresistive sensing performance, thermal insulation, and fire-retardance.

2. Experimental procedure

2.1 Chemicals and materials

Polyacrylonitrile (Mn = 150000), silicon dioxide (SiO_2, nanopowder, 10-20 nm particle size (BET), 99.5%), n-heptane (ReagentPlus, 99%), and n-Octadecyltrichlorosilane (OTS, ≥ 90%) were purchased from Merck KGaA, Darmstadt, Germany. *N, N*-Dimethylformamide (DMF, anhydrous, 99.8%) was purchased from Alfa Aesar, Thermo Fisher Scientific, UK.

2.2 Synthesis of SiCNW sponges

Precursor solutions were prepared by dissolving PAN and SiO_2 with an optimised stoichiometric ratio of C:Si = 1:1 in *N, N*-dimethylformamide (Figure S1), and stirred on a hot-plate at 80 °C for 4 h. The prepared solution was loaded into a syringe with an 18-G metal needle and delivered at a constant feed rate of 3 ml h^{-1}. A drum collector with a rotational speed of 500 rpm was placed 15 cm from the needle. A constant voltage of 20 kV (TESLAMAN TCM6000) was applied. The ambient temperature and humidity during electrospinning were controlled at ~20 °C and 40%, respectively. The thickness of the electrospun membranes was controlled by carefully regulating the depositing time of the fibres.

The electrospun PAN/SiO_2 nanofibres were collected on an Al foil and were air-cured at 270 °C for 2 h at a ramp rate of 1 °C min^{-1}. The stabilised membrane was then cut into rectangles with a dimension of 3 × 2.5 cm and stacked as a cubic sponge; an optimised pressure was applied to compact the layered structures to achieve green body (Figure S2-S4). The sample was finally sintered at 1500 °C, at a ramping rate of 5 °C min^{-1} and held for 3 h in flowing Ar atmosphere. The as-obtained SiC/C sponges were subjected to an additional thermal treatment at 800 °C for 10 min in air to eliminate the excessive carbon via oxidation.

2.3 Characterisation of SiC nanowires

The powder X-ray diffraction (XRD) patterns were recorded on a Bruker D8 Advance diffractometer with a Cu Kα radiation (λ = 0.154 nm, operated at 40 kV and 40 mA). The microstructure was examined by scanning electron microscopy (SEM) (xT Nova Nanolab

600 FIB-SEM machine) that operated at 10 kV and transmission electron microscopy (TEM) (JEM-2100, JEOL) operating at 200 kV. The elemental distribution map of single SiCNWs was obtained by EDS (Oxford Instrument System, liquid nitrogen-free SD detector, 80 mm^2, 138 eV) that fitted in TEM. The compressive mechanical test of SiCNW sponges was carried out along the membrane stacking direction on a Lloyd EZ20 advanced materials testing machine, using a 50 N detection cell and loading rate of 10 mm min^{-1}. The piezoresistive response was recorded on a KEITHLEY 6514 system sourcemeter that connected with a bespoke linear motor setup and a computer for data collection and analyses. The sample was mounted between two parallel Al plate electrodes and glued by conductive silver paste. The resistance responses were tested by applying the load on the sample along the membrane stacking direction. The high temperature testing environment is created by MOWIS 2000W professional hot air gun, which is operated under an adjustable temperature of 50-600 °C and air flow of 190 - 500 L min^{-1}. Thermal diffusivity evaluations were conducted on a NETZSCH LFA 467 HyperFlash machine in the temperature range of 25-200 °C under N_2 flow. Infrared thermal images were taken by FLIR One Pro – iOS thermal camera.

3. Results and discussion

3.1 Fabrication of SiCNW sponges.

In this study, the ultralight SiCNWs sponges were created by one-step calcination of electrospun PAN/SiO_2 nanofibre membranes that built up to sponges following the layer-by-layer stacking process. As illustrated in Figure 1, the fabrication process consists of 5 steps: dissolving PAN and SiO_2 in DMF to form composite stoke solutions, electrospinning, pre-

oxidation, cutting and stacking of the electrospun PAN-SiO_2 membranes as a 3D sponge, and finally calcination of the sponge. Benefitting from the high-speed roller collector, the as-spun PAN/SiO_2 nanofibres were uniformly aligned and distributed on the collector (Figure 1A). The as-spun PAN/SiO_2 nanofibres were then pre-oxidised in air at 270°C. During the curing process, several substantial reactions including dehydrogenation, oxidation, cyclisation of nitrile groups (C≡N) and crosslinking of the chain molecules in the form of −C=N−C=N− occurred in sequence,[15] leading to the formation of a thermally stable ladder structure,[16] which prevents the complete loss of the organic matter in the subsequent carbonisation process.[1,17,18] The PAN-SiO_2 membranes with a thickness of ~2 mm were then cut and stacked as a 3D cubic sponge with a dimension of ~3 × 2.5 × 2 cm. A pressure of 30 kPa was subsequently applied to enhance the contact between each adjacent layer. The sponge was then subjected to high temperature sintering at 1500 °C

and the carbon removal treatment, an ultralight SiCNW sponge with a density of merely 29 mg cm^{-3} was then obtained (Figure 1B).

The successful generation of SiCNWs can be ascribed to the good interaction between C- and Si-containing precursors as a result of uniform distribution of SiO_2 nanoparticles in the electrospun fibres. The generation of the SiCNW sponges that consist of the nucleation and growth of the SiCNWs is illustrated in the Figure 2A. In the first stage, with the rise of the temperature, the carbonisation of the PAN started first,[18] subsequently, according to the thermodynamic calculation (Figure S5), the SiO_2 nanoparticles that embedded in the fibres was dominantly reduced by solid phase C to provide the SiO and CO gas (Reaction (1)), they can also be reduced by CO to produce gaseous SiO and CO_2 (Reaction (2)), at low

temperatures (< 800 °C). These gaseous SiO then actively reacted with solid C to form the SiC nucleus (Reaction (3))

$$SiO_2\ (s) + C\ (s) \rightarrow SiO\ (g) + CO\ (g) \quad (1)$$

$$SiO_2\ (s) + CO\ (g) \rightarrow SiO\ (g) + CO_2\ (g) \quad (2)$$

$$SiO\ (g) + 2C\ (s) \rightarrow SiC\ (s) + CO\ (g) \quad (3)$$

In the second stage, , the continuous supply of SiO and CO gases led to the rise of their partial pressure within the confined reaction space, which eventually enabled the growth of SiC nucleus as nanowires by reaction (4).[19]

$$SiO\ (g) + 3CO\ (g) \rightarrow SiC\ (s) + 2CO_2\ (g) \quad (4)$$

Additionally, CO_2 was expected to be consumed immediately to yield gaseous CO (Reaction (5)), which increased the partial pressure of CO and promoted the growth of SiCNW.

$$CO_2\ (g) + C\ (s) \rightarrow 2CO\ (g) \quad (5)$$

All these reactions form a cycle and continuously generate abundant interconnected SiCNWs.[9]

The resulting SiCNW sponges exhibit an excellent 3D structural integrity, with each layer firmly attached; the boundary of each layer can be hardly recognised in the digital photo of the cross-sectional area (inset of Figure 2B). The SEM images of the cross-sectional area further verifies that two adjacent layers are firmly connected by the intertwined nanowires with lengths up to tens of μm, forming a porous open-cell network (Figure 2B-D). It is still worth noting that fibrous structures duplicating the original morphology of electrospun

PAN/SiO_2 fibres are identified (Figure S6), this again confirms the origination of SiCNWs from electrospun PAN/SiO_2 nanofibres.

The TEM images, together with the corresponding SAED results revealed that SiCNWs were single crystallised, growing along the [111] direction, with an interplanar spacing of the lattice fringes of 0.25 nm and some visible stacking faults (Figure 2E). The presence of Si, C, and O elements was unveiled by the EDS elementary mapping (Figure 2F), a uniform distribution of Si and C throughout the SiCNW was observed while a trace amount of O was also identified, which is believed to be formed mainly on the shell of the nanowire due to the inevitable oxidation. Figure 2G shows the XRD results of the as-electrospun PAN/SiO_2 nanofibres and resulting SiCNWs. All the diffraction peaks in the XRD pattern of SiCNWs can be indexed to the cubic SiC (JCPDS card, No. 29–1129).[9] The low intensity peak at around 33.6° represents the formation of stacking faults (S.F.),[20] in agreement of TEM images above. Whilst the broad peak between 20-30° indicate the superfluous C.

3.2 Flexibility and compressibility assessments

Due to the anisotropic lamellar deposition character of the electrospinning technique, most of the existing electrospun nanofibrous structures are just close-packed fluffy and cotton-like nanofibre membranes, which exhibit poor strength and little compressive recoverability.[14] The challenge has been overcome in this study by pre-applied pressure to electrospun PAN/SiO_2 nanofibres and the following in-situ carbothermal reaction, which establish the interconnection between adjacent layers, leading to a SiCNW network with good structural integrity. As shown in Figure 3A, the SiCNW sponge is flexible enough to be compressed

with a strain of 40% without any breakage, they could subsequently fully recover to the original shape when the load is released, which demonstrates a very good compressive recoverability. Figure 3B presents the stress-strain (σ-ε) curves at set strains of 20%, 40%, and 60%, with closed and nonlinear hysteresis loops, which is normally exhibited by highly compressive and energy-dissipative materials.[21] The loading process contains two characteristic stages: a linear elastic regime at $\varepsilon < 30\%$, yielding an elastic modulus of ~ 10.73 kPa, following a nonlinear regime with σ rising steeply, as a result of structural densification upon severe volume reduction. Unlike blow-spun TiO_2 ceramic nanofiber sponges, which exhibit stress fluctuation when compressed to 40% strain,[12] the SiCNW sponges did not show any imperfection on the stress-strain curve, implying that the majority of SiCNWs and networks in the sponge might simply experience densification process rather than structural failure.

The sponges were then subjected to 500 loading-unloading fatigue tests at a set $\varepsilon = 40\%$ (Figure 3C). During testing, the sponges did not exhibit any macroscopic crack or stress fluctuation. Compared to freeze-cast SiCNW aerogels, which lose 50% of residual stress but maintained the height of the sample after 100 loading-unloading cycles,[22] the present SiCNW sponges could retain more than 75% of the initial maximum stress and Young's modulus, as well as 89% shape recovery after 500 cycles (Figure 3D-F), suggesting excellent fatigue resistance.

The superb cyclic compressive recoverability and fatigue resistance can be accredited to: firstly, the large porosity that gives rise to more space and freedom to accommodate the deformation of the structure; secondly, the pre-applied pressure that create stubborn attachment of each adjacent layer which led to their better contact within the structure;

thirdly, the SiCNWs that generated by the carbothermal reaction are effectively bonded to each other, forming better joints rather than being loosely piled up, leading to an organised and interconnected structure.

3.3 Piezoresistivity and pressure sensing

The SiCNW sponges with a combination of compressive recoverability and fatigue resistance were further exploited as piezoresistive strain sensors (Figure S7). Figure 4A shows the variation of normalised electrical resistance ($\Delta R/R_0 = (R-R_0)/R_0$, where ΔR refers to the change of the resistance, R and R_0 represent the instantaneous resistance during testing and original resistance, respectively) of the SiCNW sponges with compression strain from 0 to 40%. The change of the relative resistance and the increase of compressive strain show a clear linear relationship, yielding a gauge factor ($GF = (\Delta R/R_0)/\Delta\varepsilon$, where $\Delta\varepsilon$ represents the variation of strain) of 1.19. A schematic in Figure 4B illustrates the mechanism of the piezoresistive sensing performance. Upon loading, SiCNWs would be compressed and bent, which made them touch and interlink with the neighbouring nanowires. Subsequently, numerous temporary knot contacts would be generated which served as shortened conduction paths through the sponge, reducing the resistance.[23] Whilst these contacts disappeared after the unloading, the resistance then returned completely to its initial value. It is believed that the superb structural integrity and compressive recoverability of the SiCNW sponges dictate the piezoresistivity of the sensing behaviour.

The cyclic piezoresistive sensing performances of the SiCNW sponges under different strains from $\varepsilon = 5\%$ to $\varepsilon = 40\%$ were explored separately. As depicted in Figure 4C, at a given frequency of 1 Hz, the relative resistance varies under different cyclic strains. However, they

exhibited outstanding strain-sensing reversibility for every stage. Meanwhile, the dependence on the frequency of the external compression has been examined. As shown in Figure 4D, under a fixed strain of 20%, the compression frequency has no effect on the piezoresistivity when the frequency was kept in the range of 1-3 Hz, however, when the testing frequency reaches 4 Hz, a noticeable unstable resistance variation output is observed, this instability and resistance variation further developed when the frequency was increased to 5 Hz. This could be ascribed to the unfinished recovery of the SiCNWs upon each cycle, i.e., dynamic recovery.

Additionally, the piezoresistive sensing capability under elevated temperatures was discovered, the high temperature environment was created using a hot-gas gun (Figure S8). As shown in Figure 4E, under 20% cyclic strain and 1 Hz frequency, the SiCNWs exhibit stable resistive variation output under temperatures of ~65.7, 99.4, and 147 °C, which became unstable when the temperature raised to 196 °C, typically when the compressive load is released. It is important to note that this imperfection can be possibly ascribed to the change of the electrical conductivity of the electrodes/conductive paste or the failure of the conductive paste, which melted under high temperatures and elevated air flow velocity, causing the partial detachment between the sample and the electrodes. However, the SiCNW sponge sensor still displays a much broader allowed working temperature range than existing polymer-based sensors.[24] It can be asserted that the SiCNW sponges could indeed provide excellent sensing performance under a variety of complex environments.

Furthermore, based on the excellent cyclic compression behaviour of the sponges that present earlier, the long-term cyclic compression was also performed to assess the repeatability and durability of the sensor. Figure 4F displays the representative electrical resistance variations

under 2000 compressive loading-unloading cycles at a strain of 20% and a frequency of 1 Hz. The SiCNW sponges exhibited superb stability with a consistent response. When the test was carried out at a strain of 30%, the SiCNW sponges present similar excellent repeatability with negligible drift and fluctuation (Figure 4G). In stark contrast to the polymer-MWNTs composites sensors who suffer evident drift during the test due to the aggregation of the carbon phase,[25] the present results convincingly suggest that the SiCNW sponges are superior in terms of repeatability and durability.

3.4 Thermal insulation performance and fire-retardance

The thermal conductivity as a density-related property essentially depends on the porosity of a given material, since the pores act as obstacles against thermal transfer by scattering the phonon transport.[26,27] Owing to their ultralight density of 29 mg cm^{-3}, the SiCNW sponges therefore exhibit a thermal conductivity of merely 24 mW $m^{-1}K^{-1}$ at ambient conditions, even lower than air (Figure 5A).[28] Such an ultralow thermal conductivity can be also accredited to strong boundary scattering from nanowire structures and enhanced photo-defect scattering caused by the stacking faults in the SiCNWs.[29] As summarised in Table S1, the SiCNW sponges possess very similar thermal conductivities, as compared to other ultralight or even flyweight aerogels. This comparison implies that these SiCNW sponges are a promising candidate for super thermal insulators. Furthermore, they exhibit temperature-invariant thermal conductivity. With the escalation of the test temperature from 25 to 200 °C, there was only a slight rise in the conductivity, which is due to the increased thermal convection at high temperatures.[30] This result suggests that the effect of the temperature on the thermal conductivity of the material is very small.

As a proof of concept for the thermal insulation application, the transient temperature response behaviour of the SiCNW sponges at different conditions were evaluated by a thermal infrared imager. The sponge was placed on a hot plate with the temperature of 200 °C and the temperature distributions of the materials were recorded. As shown in Figure 5B, the SiCNW sponge showed a gentle increase in temperature from the bottom to top, the temperature at the top was 25.5 °C after being heated for 30 s, which became 39.4 °C 10 min later, and finally reached 61.2 °C after 30 min. As shown in Figure 5C, when placed on top of a cooling stage with temperature < -20 °C, the top part of the sponge maintained a temperature of 19.4 °C after 10 min, still very close to ambient temperature, reflecting a good warmth retention. To further demonstrate the thermal insulation performance, a fresh flower was placed on top of a SiCNW sponge to examine the capability of SiCNW sponge for protecting the fresh flower under heating (Figure 5D). It can be observed that after heating for 10 min, the flower remained fresh with negligible withering or carbonisation, highlighting the excellent thermal insulation behavior of the SiCNW sponges in a wide temperature range. Additionally, as shown in Figure 5E, the sponge can be compressed at $\varepsilon = 40\%$ and recovered rapidly to the original shape in butane blowtorch flame at 1300 °C, no ignition or structural change was observed, demonstrating simultaneous superb fire-retardance and temperature-invariant recoverability. Such good performance can be ascribed to: (1) The intrinsic thermal-oxidation resistance of SiC as a carbide ceramic (Figure S9); (2) The robust and interconnected porous architecture which can distribute the induced thermal stress very well;[31] (3) The formation of SiO_2 layer on the surface of SiCNWs due to passive oxidation leads to a synergetic protection of the inner region from further oxidation.[32]

The thermal conductivity and maximum allowed working temperatures of typical thermal insulating materials have been summarised in Figure 5F. Comparted to ultralight networks

made of polymers,[33] cellulose-based composites,[34] carbon,[35] conventional SiO_2 fiber,[36] and fiberglass wool,[37] who either suffer from poor high-temperature stability or inflammability, the present SiCNWs sponges offer a combination of low thermal conductivity and high maximum allowed working temperatures up to 1300 °C, making them promising candidate as thermal insulator or harsh-environment applications.

4. Conclusion

In summary, based on a special electrospinning-calcination (carbothermal reduction) concept, we successfully generated ultralight 3D SiCNW sponges by simply staking and sintering electrospun PAN/SiO_2 nanofibre membranes. The resulting sponges, made of well-bonded interconnected SiCNWs, exhibited superb recoverability and excellent fatigue resistance. The unique combination of excellent mechanical properties and the piezoresistive behaviour of the SiCNW sponges enabled them to detect mechanical strains at various complex conditions, acting as a promising sensor candidate for the fabrication of electromechanical device. The ultralow density (29 mg cm^{-3}) endows the sponges with superb insulation performance, with a thermal conductivity of only 24 mW $m^{-1}K^{-1}$ at room temperature. Furthermore, the sponges demonstrate simultaneously excellent fire-retardance and temperature-invariant recoverability. The multifunctionality exhibited by such sponges could also find many engineering applications, particularly for harsh environments. This present technique demonstrates much enhanced efficiency, flexibility, and possibility for large-scale production, which may be extended to the fabrication of a wide variety of advanced ultralight ceramic nanowire sponges.

Acknowledgement

Thank the EPSRC for Financial support (EP/P003435/1)

References

1. Leventis N, Sadekar A, Chandrasekaran N, Sotiriou-Leventis C. Click synthesis of monolithic silicon carbide aerogels from polyacrylonitrile-coated 3D silica networks. Chem Mater. 2010;22(9):2790–2803.

2. Lee JS, Lee SH, Choi SC. Improvement of porous silicon carbide filters by growth of silicon carbide nanowires using a modified carbothermal reduction process. J Alloys Compd. 2009;467(1–2):543–549.

3. Su L, Wang H, Niu M, Fan X, Ma M, Shi Z, Guo SW. Ultralight, recoverable, and high-temperature-resistant SiC nanowire aerogel. ACS nano. 2018;12(4):3103–3111.

4. Su L, Wang H, Jia S, Dai S, Niu M, Ren J, Lu X, Cai Z, Lu D, Li M, Xu L, Guo, SW, Zhuang L, Peng, K. Highly stretchable, crack-insensitive and compressible ceramic aerogel. ACS nano. 2021;15(11):18354–18362.

5. Li B, Yuan X, Gao Y, Wang Y, Liao J, Rao Z, Mao B, Huang H. A novel SiC nanowire aerogel consisted of ultra long SiC nanowires. Mater Res Express. 2019;6(4):045030

6. Yao B, Lu B, Huang Q, Huang ZR, Yuan Q. The preparation of SiC ultrafine fibers containing low amount of oxygen by the electrospinning and pyrolysis of vinyl-modified polycarbosilane. Ceram Int. 2020;46(7):357–362.

7. Khishigbayar KE, Joo YJ, Cho KY. Microwave-assisted heating of electrospun SiC fiber mats. J Korean Ceram Soc. 2017;54(6):499–505.

8. Kim TE, Bae JC, Cho KY, Shul YG, Kim CY. Fabrication of electrospun SiC fibers web/phenol resin composites for the application to high thermal conducting substrate. J Nanosci Nanotechnol. 2013;13(5):3307–3312.

9. Wei J, Li X, Wang Y, Chen B, Zhang M, Qin C. Photoluminescence property of inexpensive flexible SiC nanowires membrane by electrospinning and carbothermal reduction. J Am Ceram Soc. 2020;103(11):6187–6197.

10. Wang B, Sun L, Wu N, Wang Y. Combined synthesis of aligned SiC nanofibers via electrospinning and carbothermal reduction. Ceram Int. 2017;43(13):10619–10623.

11. Jia C, Li L, Liu Y, Fang B, Ding H, Song J, Liu Y, Xiang X, Lin S, Li Z, Si W, Li B, Sheng X, Wang D, Wei X, Wu H. Highly compressible and anisotropic lamellar ceramic sponges with superior thermal insulation and acoustic absorption performances. Nat Commun. 2020; 11(1):1−13.

12. Wang H, Zhang X, Wang N, Li Y, Feng X, Huang Y, Zhao C, Liu Z, Fang M, Ou G, Gao H, Li X, Wu H. Ultralight, scalable, and high-temperature–resilient ceramic nanofiber sponges. Sci Adv. 2017;3(6):e1603170.

13. Ferraro C, Garcia-Tuñon E, Rocha VG, Barg S, Fariñas MD, Alvarez-Arenas TEG, Sernicola G, Giuliani F, Saiz E. Light and strong SiC networks. Adv Funct Mater. 2016;26(10): 1636−1645.

14. Zhang M, Wang Y, Zhang Y, Song J, Si Y, Yan J, Ma C, Liu YT, Yu J, Ding B. Conductive and elastic TiO_2 nanofibrous aerogels: a new concept toward self–

supported electrocatalysts with superior activity and durability. Angew Chemie. 2020;59(51):23252–23260.

15. Nataraj SK, Yang KS, Aminabhavi TM. Polyacrylonitrile-based nanofibers—A state-of-the-art review. Prog Polym Sci. 2012;37(3):487–513.

16. Khayyam H, Jazar RN, Nunna S, Golkarnarenji G, Badii K, Fakhrhoseini SM, Kumar S, Naebe M. PAN precursor fabrication, applications and thermal stabilization process in carbon fiber production: Experimental and mathematical modelling. Prog Mater Sci. 2020;107:100575.

17. Zhou Z, Lai C, Zhang L, Qian Y, Hou H, Reneker DH, Fong H. Development of carbon nanofibers from aligned electrospun polyacrylonitrile nanofiber bundles and characterization of their microstructural, electrical, and mechanical properties. Polymer. 2020;50(13):2999–3006.

18. Arshad SN, Naraghi M, Chasiotis I. Strong carbon nanofibers from electrospun polyacrylonitrile. Carbon. 2011;49(5):1710–1719.

19. Chu Y, Jing S, Chen J. In situ synthesis of homogeneously dispersed SiC nanowires in reaction sintered silicon-based ceramic powders. Ceram Int. 2018;44(6);6681–6685.

20. Zhang M, Zhao J, Li Z, Yu H, Wang Y, Meng A, Li Q. Bamboo-like 3C-SiC nanowires with periodical fluctuating diameter: Homogeneous synthesis, synergistic growth mechanism, and their luminescence properties. J Solid State Chem. 2016;243:247–252.

21. Ren B, Liu J, Rong Y, Wang L, Lu Y, Xi X, Yang, J. Nanofibrous aerogel bulk assembled by cross-linked SiC/SiOx core–shell nanofibers with multifunctionality and temperature-invariant hyperelasticity. ACS Nano. 2019;13(10):11603–11612.

22. Su L, Wang H, Niu M, Dai S, Cai Z, Yang B, Huyan H, Pan X. Anisotropic and hierarchical SiC@SiO_2 nanowire aerogel with exceptional stiffness and stability for thermal superinsulation. Sci Adv. 2020;6(26):eaay6689.

23. Chen Y, Ola O, Chen H, Wang N, Xia Y, Zhu Y. SiC nanowire sponges as electropressure sensors. ACS Appl Nano Mater. 2019;2(12):7540–7548.

24. Liu H, Chen X, Zheng Y, Zhang D, Zhao Y, Wang C. Lightweight, superelastic, and hydrophobic polyimide nanofiber/MXene composite aerogel for wearable piezoresistive sensor and oil/water separation applications. Adv Funct Mater. 2021;31(13):2008006.

25. Rizvi R, Cochrane B, Biddiss E, Naguib H. Piezoresistance characterization of poly (dimethyl-siloxane) and poly (ethylene) carbon nanotube composites. Smart Mater Struct. 2011;20(9):094003.

26. Chen Y, Wang N, Ola O, Xia Y, Zhu Y. Porous ceramics: Light in weight but heavy in energy and environment technologies. Mater Sci Eng R. 2021;143:100589,

27. Bergman TL, Incropera FP, Dewitt DP, Lavine AS. Fundamentals of heat and mass transfer. John Wiley & Sons, 2011.

28. Engineering ToolBox. Air - Thermal Conductivity vs. Temperature and Pressure. 2009.

https://www.engineeringtoolbox.com/air-properties-viscosity-conductivity-heat-capacity-d_1509.html (assessed 26 Septermber 2021)

29. Lu D, Su L, Wang H, Niu M, Xu L, Ma M, Gao H, Cai Z, Fan X. Scalable fabrication of resilient SiC nanowires aerogels with exceptional high-temperature stability. ACS Appl Mater Interfaces. 2019;11(48):45338–45344.

30. Wang F, Dou L, Dai J, Li Y, Huang L, Si Y, Yu J, Ding B. In situ synthesis of biomimetic silica nanofibrous aerogels with temperature–invariant superelasticity over one million compressions. Angew Chemie. 2020;132(21):8362–8369.

31. Yang R, Hu F, An L, Armstrong J, Hu Y, Li C, Huang Y, Ren S. A hierarchical mesoporous insulation ceramic. Nano Lett. 2020;20(2):1110–1116.

32. Zhang L, He P, Song K, Zhang J, Zhang B, Huang R, Zhang Q. Three-dimensional graphene hybrid SiO_2 hierarchical dual-network aerogel with low thermal conductivity and high elasticity. Coatings. 2020;10(5):1–13.

33. Verdolotti L, Lavorgna M, Lamanna R, Di Maio E, Iannace S. Polyurethane-silica hybrid foam by sol–gel approach: Chemical and functional properties. Polymer. 2015;56:20–28.

34. Zhang J, Cheng Y, Tebyetekerwa M, Meng S, Zhu M, Lu Y. “Stiff–soft” binary synergistic aerogels with superflexibility and high thermal insulation performance. Adv Funct Mater. 2019;29(15):1806407.

35. Lu X, Nilsson O, Fricke J, Pekala RW. Thermal and electrical conductivity of monolithic carbon aerogels. J Appl Phys. 1993;73(2):581–584.

36. Huang Y, He S, Chen G, Shi X, Yang X, Dai H, Chen X. Mechanical reinforced fiber needle felt/silica aerogel composite with its flammability. J Sol-Gel Sci Technol. 2018;88(1):129–140.

37. Jelle BP. Traditional, state-of-the-art and future thermal building insulation materials and solutions–Properties, requirements and possibilities. Energy Build. 2011;43(10):2549–2563.

Figure 1 Schematic of preparation of SiCNWs sponges. (A) Electrospinning of PAN/SiO_2 fibres. (B) Thermal cure of the electrospun fibres, assembly of the 2D membrane as a 3D sponge, and high temperature calcination. The resulting SiCNW sponge can be easily propped by a dandelion.

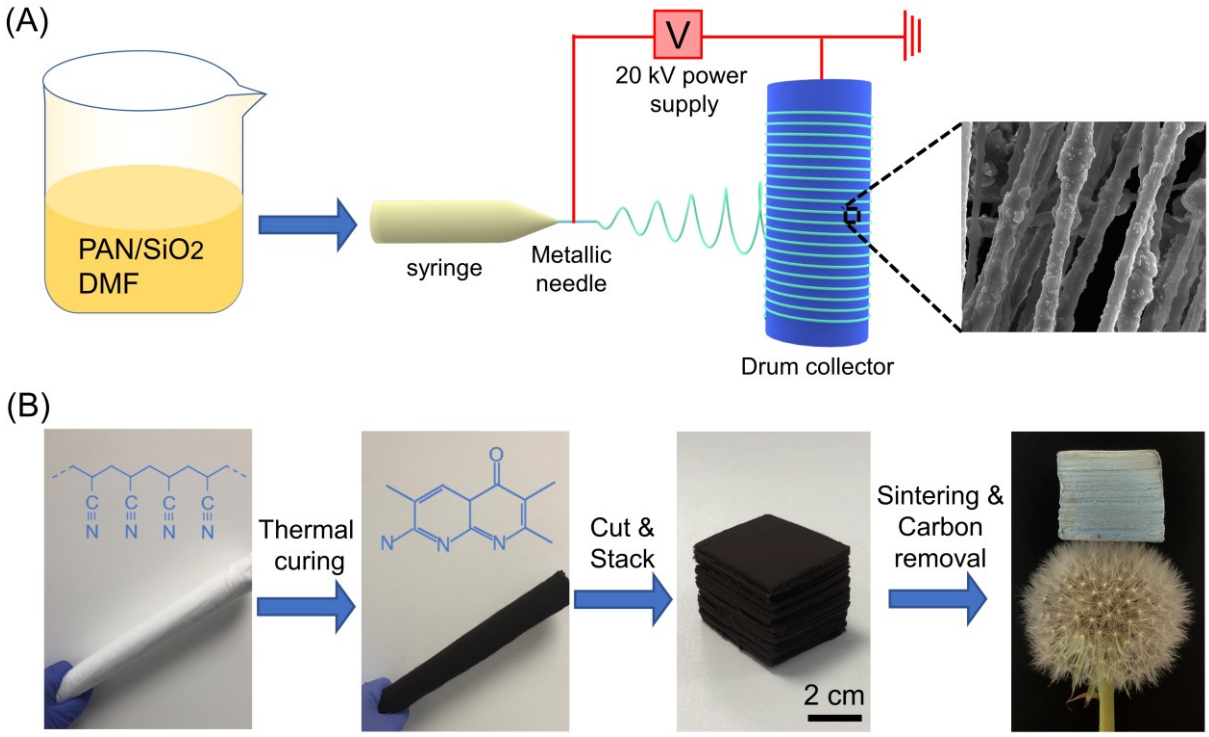

Figure 2 (A) Schematics of the transformation of the PAN/SiO_2 nanofibre sponge to SiCNW sponge; (B-D) SEM images of the cross-sectional area of SiCNW sponge, the boundary between two adjacent layers is indicated by the arrows; (E) TEM image (inset is the SAED pattern); (F) TEM images of a SiCNW and the corresponding elemental maps of Si, C, and O; and (G) XRD profile of SiCNW.

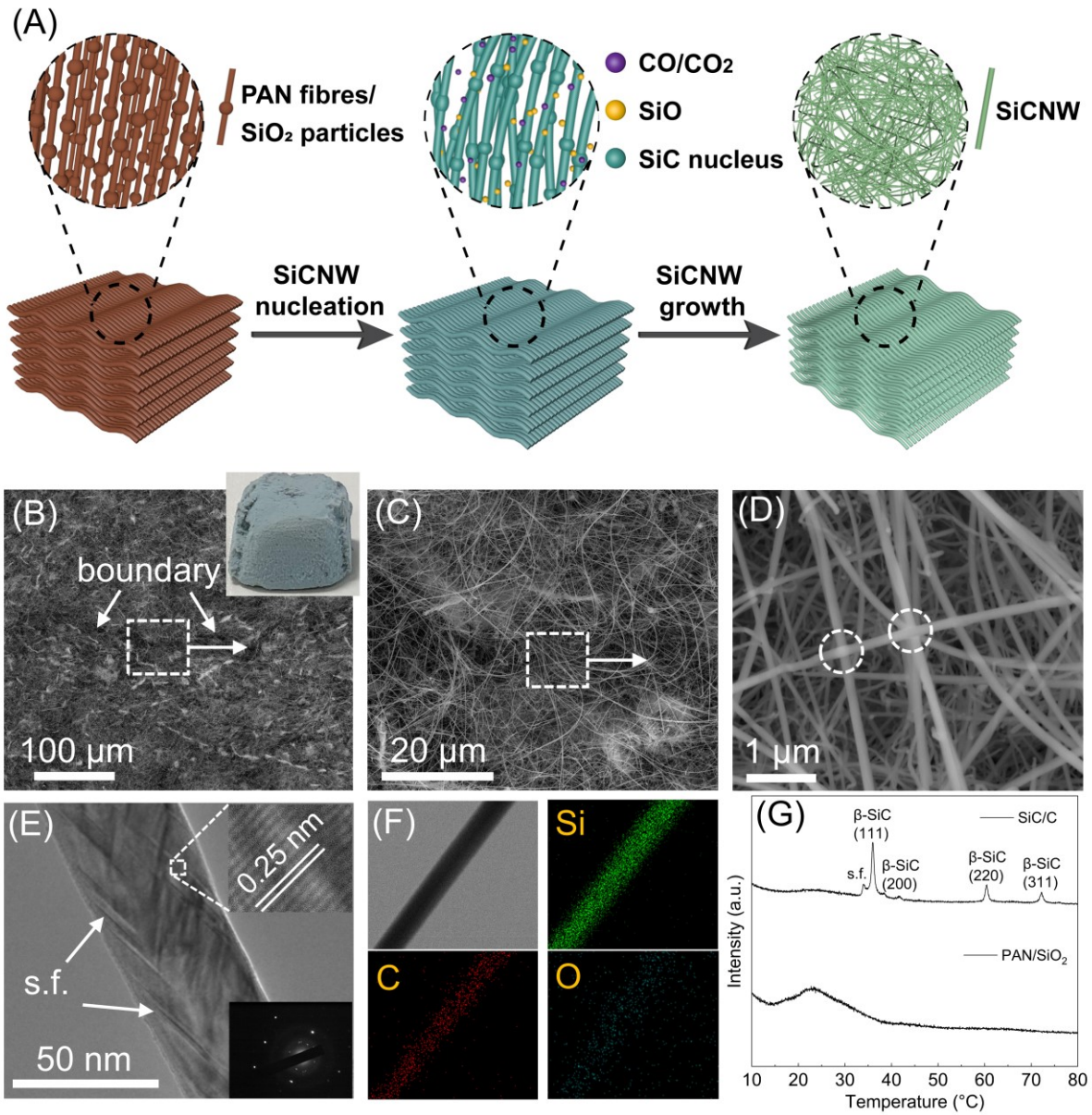

Figure 3 (A) Photos showing the high compressibility of the SiCNW sponges. (B) Compressive stress-strain curves of the SiCNW sponges at set strains of 20%, 40%, and 60%. (C) Stress-strain curves; (D) Maximum stress; (E) Young's modulus; and (F) Strain retention during 500 loading-unloading cycles at set ε = 40%.

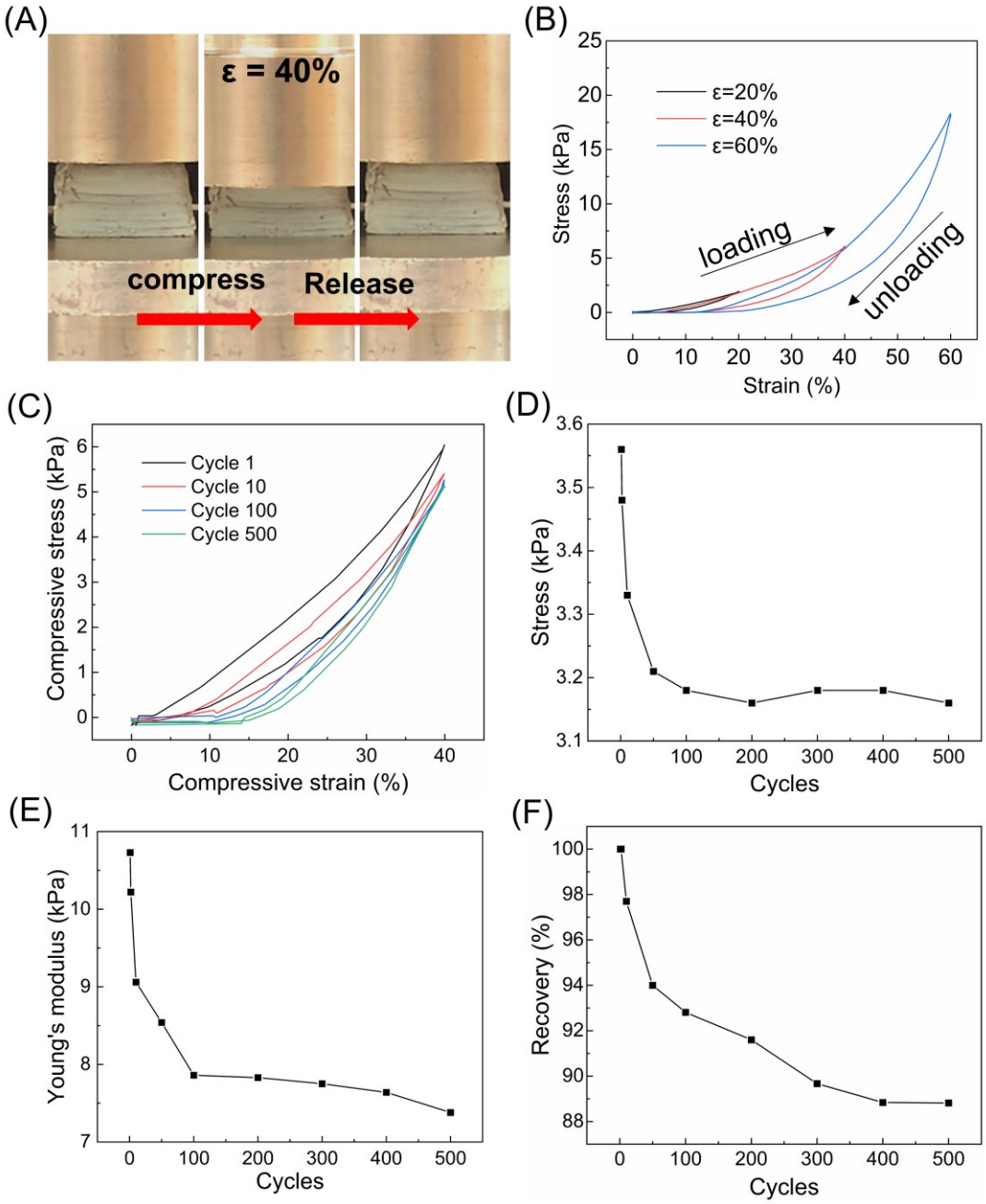

Figure 4 (A) Variation of electrical resistance against strains under compression. Gauge factors were derived from the linear fitting. (B) Schematic depiction of the SiCNW sponges as a piezoresistive strain sensor. Cyclic piezoresistive sensing performance of the SiCNW sponges (C) under different compressive strain/pressure levels at a fixed frequency of 1 Hz; (D) under different compression frequency at fixed ε = 20%; and (E) at elevated temperatures. Electrical resistance variation of SiCNW sponges (F) up to 2000 compressing cycles under ε = 20% and frequency of 1 Hz and (G) up to 1000 compressing cycles under ε = 30% and frequency of 1 Hz.

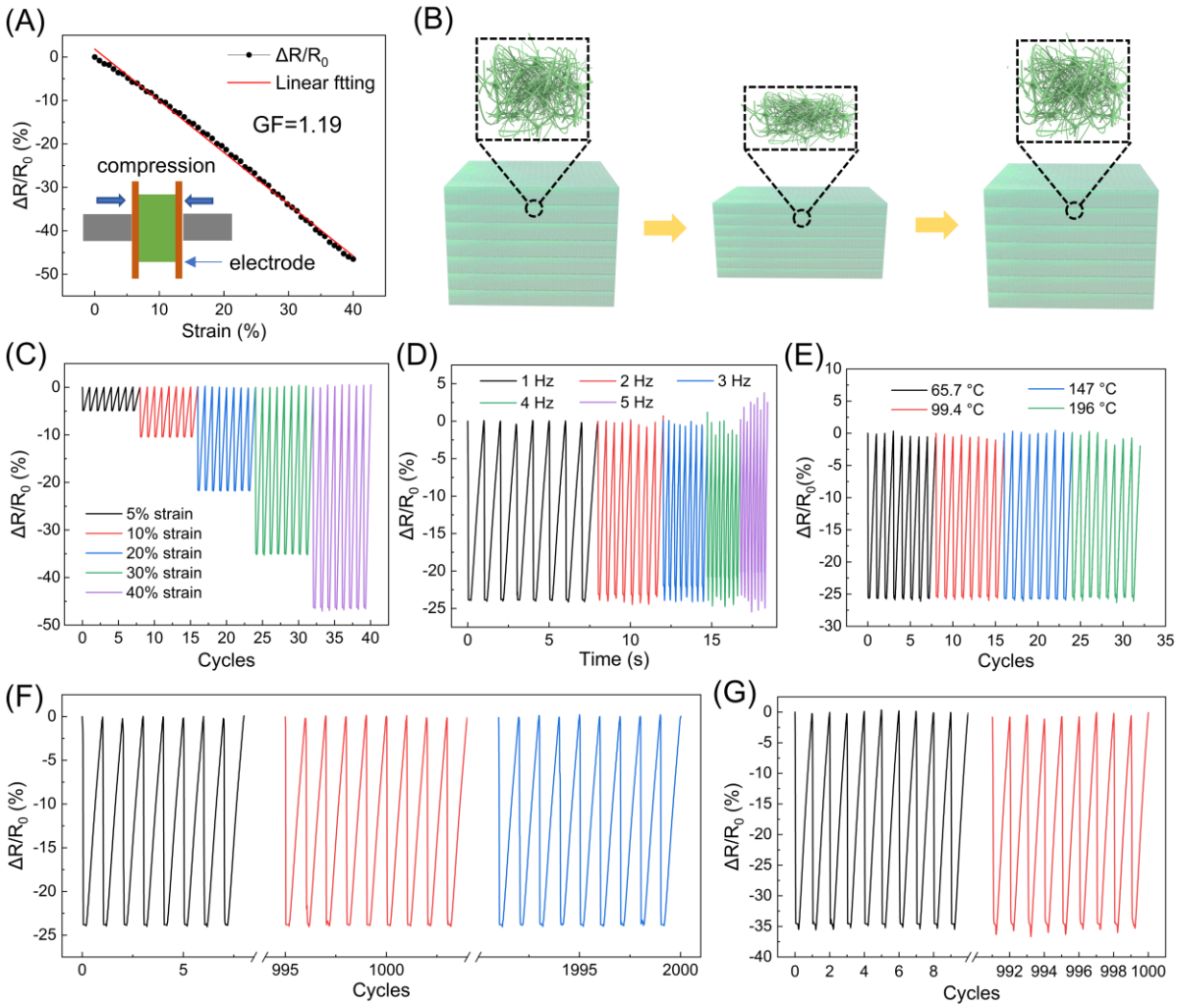

Figure 5 (A) Thermal conductivity of the electrospun SiCNW sponges against air, as a function of temperature. Infrared thermal images of a SiCNW sponge (B) on a stable hot plate at 200 °C during the 30 min heating process, and (C) on a stable cold finger with temperature < -20 °C for 10 min. (D) Digital photos showing the SiCNW sponge protects the fresh flower under heating by the alcohol lamp for 10 min. (E) Photographs showing compression-recovery process of the SiCNW sponges exposed to the flame of a butane blow torch. (F) Thermal conductivity versus the maximum working temperatures for existing ultralight nanostructured materials.